CHAPTER 6

FRACTAL BOUNDARIES

Fractal boundaries are very important in the applications of discrete dynamics. First we describe in greater detail the basic features of contact bifurcations, which we have encountered already in Chapter 5, with a sequence of hand drawings. Then we will go on to an exemplary bifurcation sequence with computer graphics, in which the fractal implications of these contact events for the boundaries become clear.

6.1 CONTACT BIFURCATION CONCEPTS

We now introduce the simplest kinds of contact bifurcations, which are global bifurcations in the sense that the topology of the basins changes.

6.1.1 The loss of simple connectivity

First we show the transition of a basin D from simple to multiple connectedness due to the appearance of holes in D. In Figure 6-1, D (shown shaded) is simply connected; there are no holes. In Figure 6-2, a contact occurs at the point h_0 between $\mathcal{F}$, the frontier of D, and L (also denoted L_0 in the figures), the critical curve of rank 1. The rank 1 preimage of h_0 is a point, h_{-1}, of L_{-1} belonging to D. This point and all of its preimages are germs of holes; they become holes after the crossing of $\mathcal{F}$ through L.

In Figure 6-3, after the crossing of $\mathcal{F}$ and L, the sector H_0 has a rank 1 preimage in the hole H_{-1}, and this hole no longer belongs to D, nor do its preimages.

FIGURE 6-1.

The shaded region is the basin, D. The two fixed points are labelled P and Q.

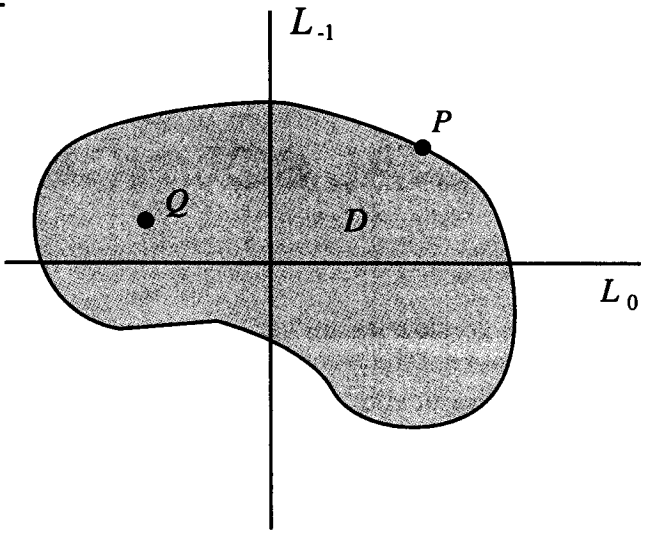

FIGURE 6-2.

A contact occurs at a single point.

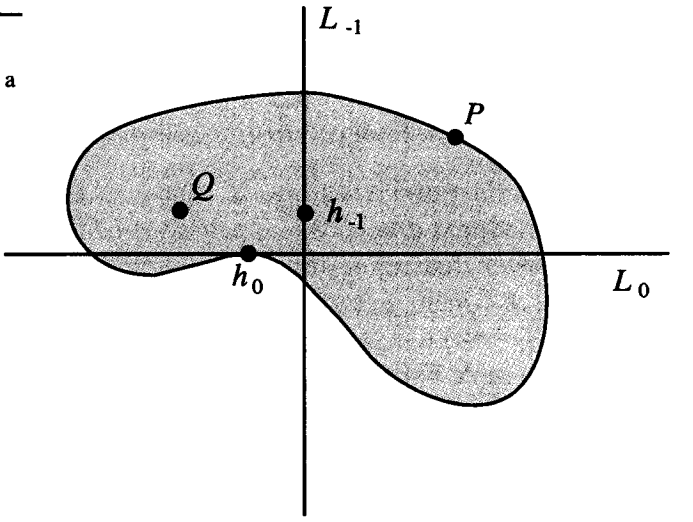

FIGURE 6-3.

The two contact points border the main hole, shown here with its preimages (holes) of ranks 1, 2, and 3.

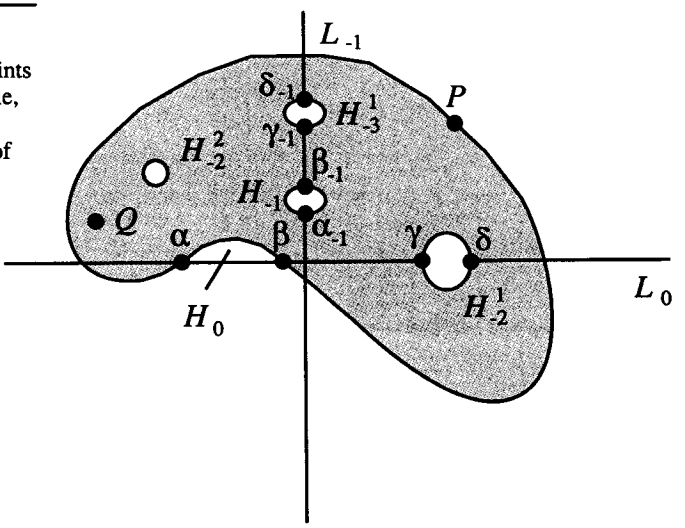

6.1.2 The loss of connectedness

Next, we show the transition of a basin D from connectedness to disconnectedness; that is, from one to many pieces.

In Figure 6-4, the basin D is connected. In Figure 6-5, a contact between $\mathcal{F}$ and L occurs at the point h_0 of L. Its rank 1 preimage h_{-1} in L_{-1}, and all the preimages of h_{-1}, are outside of D. They are germs of components of D (*islands*), and become islands after the crossing of $\mathcal{F}$ through L.

In Figure 6-6, after the crossing of $\mathcal{F}$ and L, the sector (*headland*) Δ_0 has a rank 1 preimage in the island D_{-1}. This island belongs to D, as do its preimages. In this case the component of the basin D containing the attractor is called the *immediate basin*, D_0.

FIGURE 6-4.

The shaded region is the basin, D.

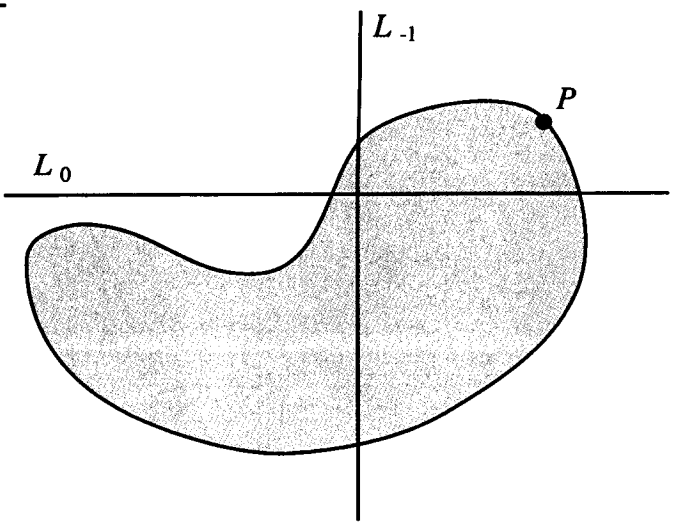

FIGURE 6-5.

Contact is made at a single point.

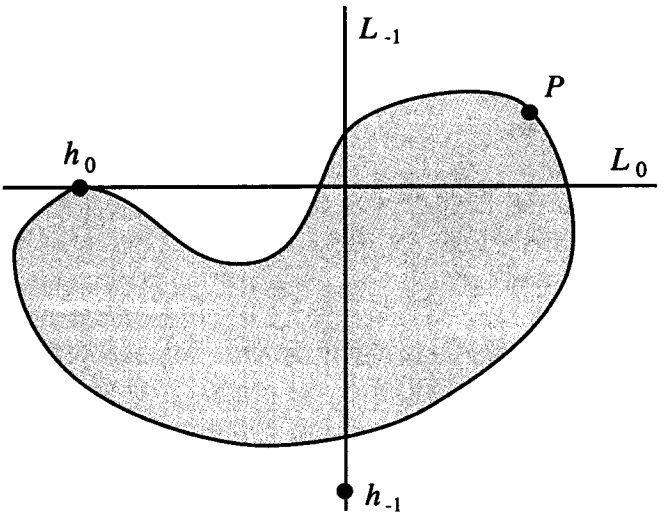

FIGURE 6-6.

The two points of contact border a headland, shown here darkly shaded. One preimage (island) is also shown.

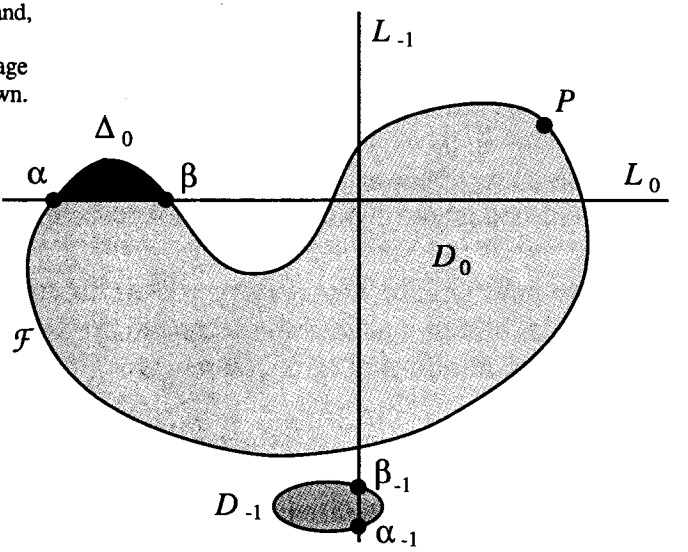

6.1.3 Distinguishing two types of contact bifurcation

Now we must assume the notions of open and closed subsets of the plane, as presented in advanced calculus, for example. Recall that the *closure* of a subset of the plane, S, is the smallest closed set containing S, for which we use the notations $cl(S) = \bar{S}$. The *boundary* of a subset S of the plane is defined as the common points of the closure of S and the closure of the complement of S; that is $bd(S) = \partial S = \bar{S} \cap cl(R^2 \backslash S)$.

The two types of contact bifurcation shown in 6.1.1 and 6.1.2 are similar, but are distinguished by the behavior of the point h_{-1} of L_{-1}. In these two cases, Figure 6-2 and Figure 6-5, we may see two simple rules.

- If the point h_{-1} belongs to the portion of L_{-1} inside $cl(D)$, then holes will appear.

- On the other hand, if h_{-1} belongs to the part of L_{-1} outside of $cl(D)$, then islands will appear.

Note: A basin is an open set, that is, every point of D has a neighborhood contained entirely within D. Also, a basin is backwards invariant, that is, all preimages of a point of D belong to D, and in fact, $T^{-1}(D) = D$. Generally, the boundary of a basin, $\mathcal{F} = bd(D)$, is backwards invariant; but there are exceptions, and Figures 6-2 and 6-5 both show this invariance violated, if $\mathcal{F}$ is considered as the boundary of the unbounded basin surrounding D in Figure 6-2 and the boundary of the bounded basin D in Figure 6-5. As we are interested in describing the bifurcation of the bounded basin we may use the two following bifurcation rules:

- When $T^{-1}(\mathcal{F}) \setminus \mathcal{F}$ belongs to $cl(D)$ at a contact bifurcation, then holes will appear.
- When $T^{-1}(\mathcal{F}) \setminus \mathcal{F}$ does not belong to $cl(D)$, then islands will appear.

Notice that the transition from $T^{-1}(\mathcal{F}) = \mathcal{F}$ to $T^{-1}(\mathcal{F}) \pi\pi\pi \neq \mathcal{F}$ can occur only if for some point of $\mathcal{F}$, the number of preimages increases. Recall that the preimages of a point x can increase only by the crossing of x through L. Thus, these bifurcations of a basin must involve a contact between $\mathcal{F}$ and L.

If h_0 in L is a point of contact between $\mathcal{F}$ and L, and h_{-1} is its unique rank 1 preimage belonging to L_{-1}, then the iterated preimages (that is, of rank 1, rank 2, and so on) of h_{-1} may be finite in number (ending in a point with no preimages), or infinite within a finite number of sequences (due to some points having a finite number of preimages of rank 1), or even infinite with an infinite number of sequences (due to some point having an infinite number of preimages of rank 1), and chaotic.

Warning: The simple rules described above are only sufficient conditions for the appearance of holes or islands. We will see soon that contact bifurcations causing the appearance of holes or islands may occur even without exception to the general situation, $T^{-1}(\mathcal{F}) = \mathcal{F}$. This situation arises in bifurcations involving the reunion of holes or islands, as described in the following figures.

6.1.4 Further contacts

The first three drawings, Figures 6-7, 6-8, and 6-9, are the same as Figures 6-4, 6-5, and 6-6. After Figure 6-9, the components of the disconnected basin, which are given by the preimages of the headland, Δ_0, increase and come together, touching in Figure 6-10. Their reunion after this bifurcation is shown in Figure 6-11.

The points of the arc of the frontier $\mathcal{F}_0$ of D_0 external to the boundary of the headland F_i have preimages which belong to the immediate basin D_0 in Figure 6-9.The points of F_i have preimages in the boundaries of the other components of the total basin, D.

In Figure 6-10, the boundary of the immediate basin and the boundary of the main component, D_{-1}, have contact at the point k_{-1}, which belongs to $\mathcal{F}_0$, to the boundary of D_{-1}, and to the critical curve L_{-1}. All preimages previously disjoint now have a contact point in the preimages of k_{-1}.

In Figure 6-11, after this contact bifurcation, all of the former components have been reunited.

Note: Beginning with the disconnected basin of Figure 6-9, a bifurcation sequence might proceed either through Figure 6-8 to Figure 6-7, with the components decreasing and disappearing, or through Figure 6-10 to Figure 6-11, with the components increasing and reuniting. A similar sequence might occur with holes (islands) as follows.

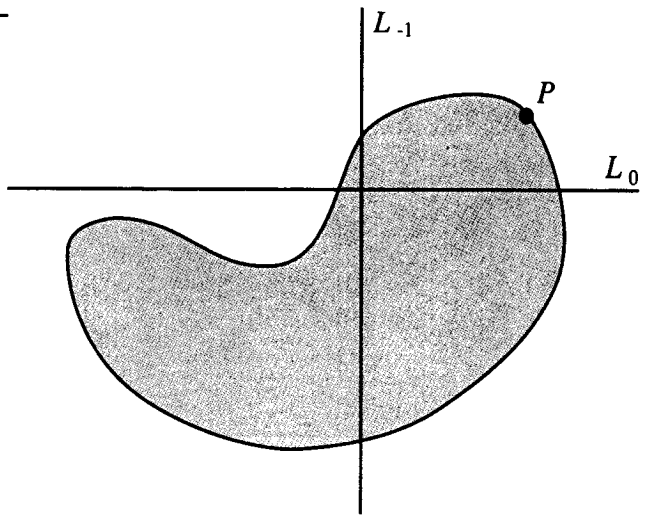

FIGURE 6-7.

Compare with Figure 6-4.

FIGURE 6-8.

Compare with Figure 6-5.

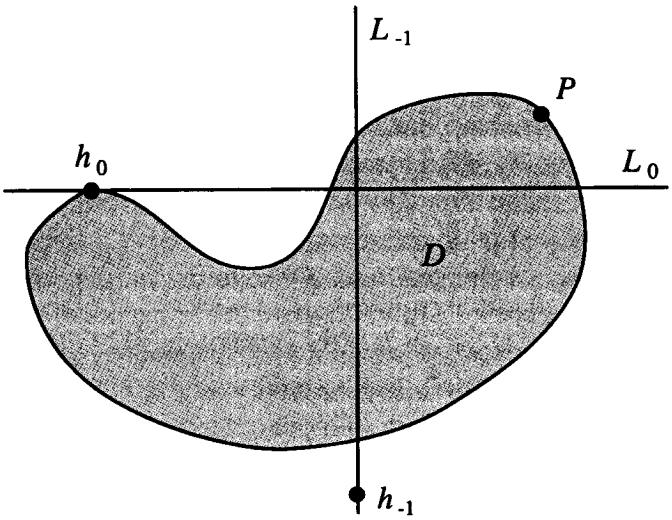

FIGURE 6-9.

Compare with Figure 6-6. Here is a headland, darkly shaded, and its preimage, an island.

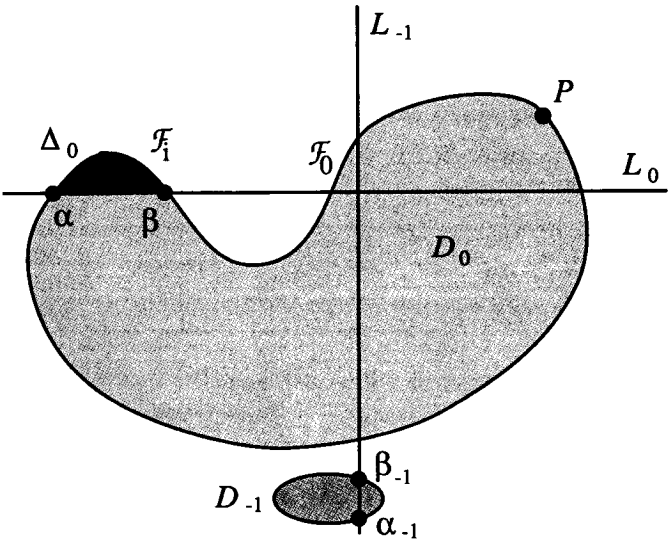

FIGURE 6-10.

Here is a new point of contact at one end of the headland, and another on the island.

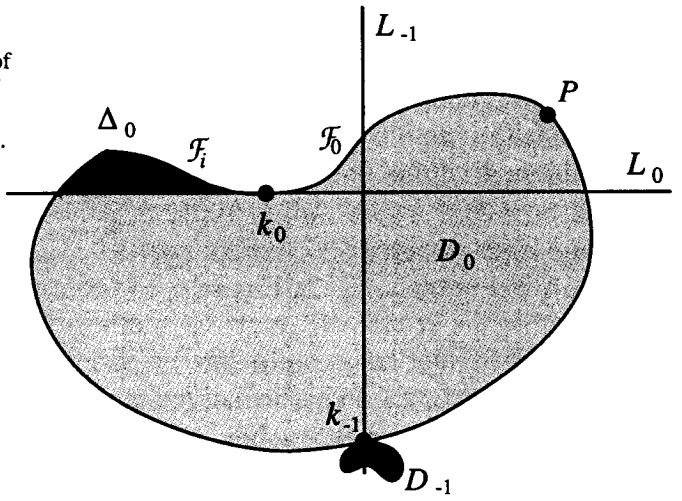

FIGURE 6-11.

The island has rejoined the mainland.

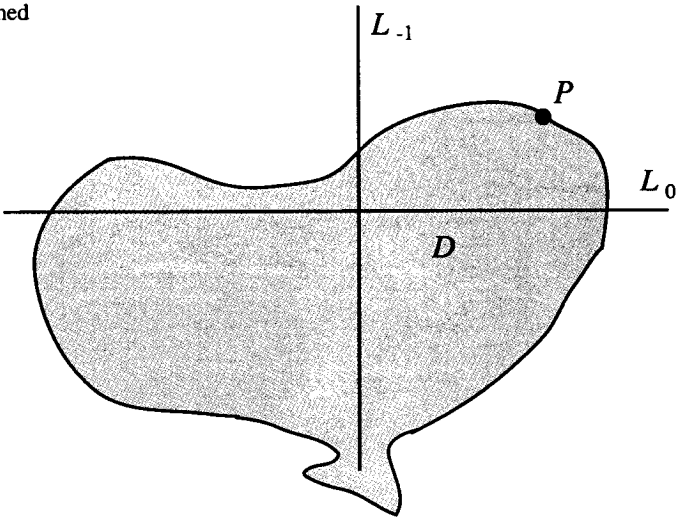

6.1.5 An alternative contact scenario

Figures 6-12, 6-13, and 6-14 are identical to Figures 6-1, 6-2, and 6-3 of this chapter. As the bifurcation sequence progresses, the holes inside the basin D increase and get closer together.

In Figure 6-14, the preimages of the points in $\mathcal{F}_e$ belong to the external boundary, while the preimages of the points of $\mathcal{F}_i$ (the boundary of H_0) belong to the boundaries of the internal holes, called internal boundaries. In Figure 6-15, all the holes which are preimages of the sector H_0 meet in another contact bifurcation. The external frontier has met the internal frontier, due to the point of tangency with L, k_0. In particular, the main hole, H_{-1}, has made contact with the external frontier, $\mathcal{F}_e$, at the point k_{-1}, which belongs to $\mathcal{F}_e$, to the boundary of H_{-1}, and to L_{-1}. In Figure 6-16, after the bifurcation, all the holes have disappeared due to the contact in Figure 6-15, by opening to the sea outside.

Note: Beginning with the multiply-connected basin of Figure 6-14, a bifurcation sequence might proceed either through Figure 6-13 to Figure 6-12, with the holes decreasing and disappearing, or through Figure 6-15 to Figure 6-16, with the holes increasing and reuniting. Also note that the sequence of Figures 6-12 to 6-16, viewed from the complementary basin, $D(\infty)$, is analogous to the sequence of Figures 6-7 to 6-11.

FIGURE 6-12.

Like Figure 6-1.

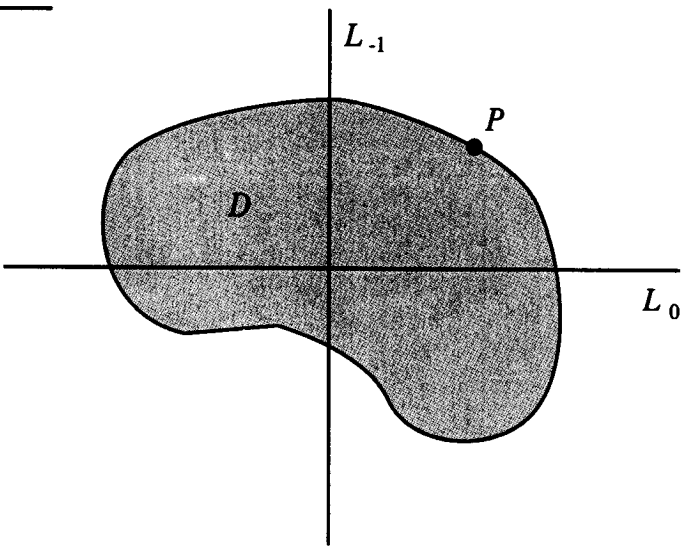

FIGURE 6-13.

Like Figure 6-2.

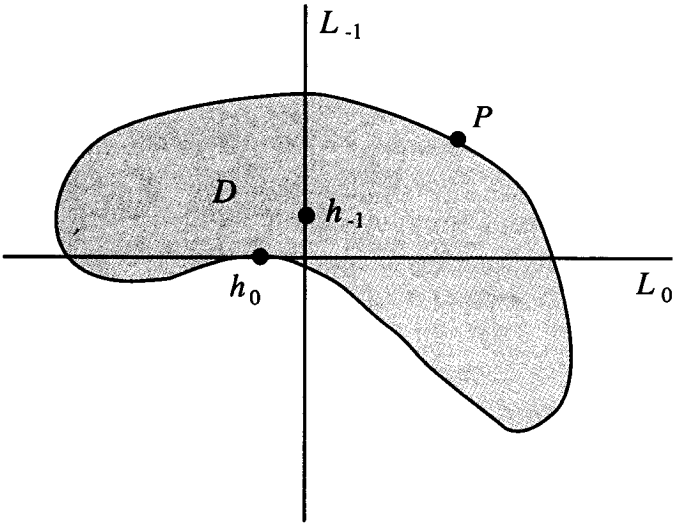

FIGURE 6-14.

Like Figure 6-3.

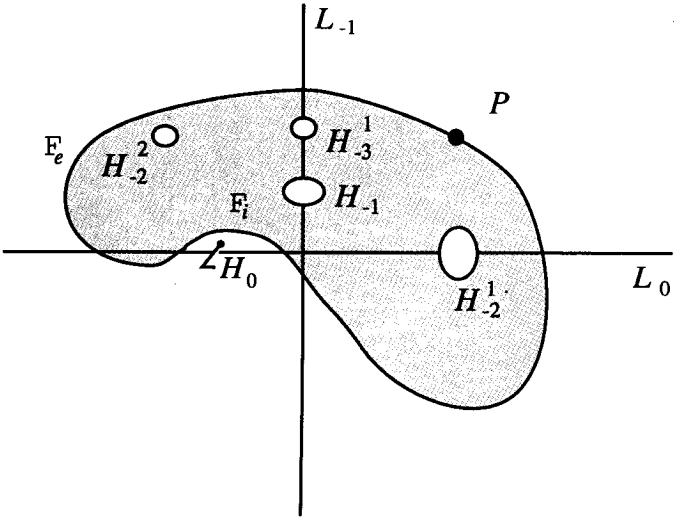

FIGURE 6-15.

A contact of holes.

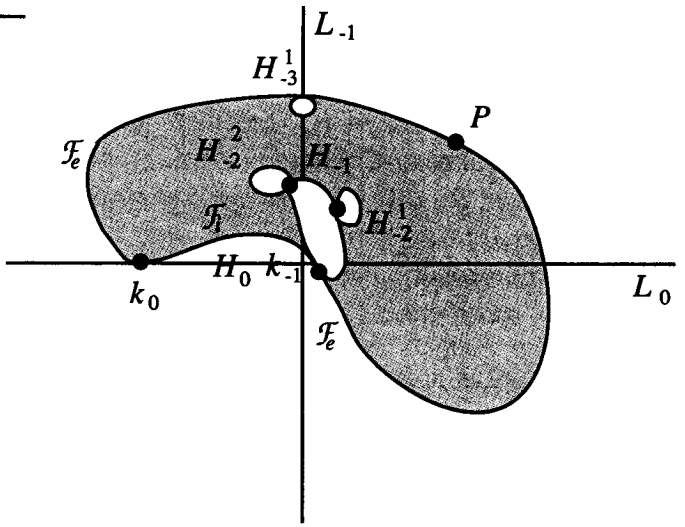

FIGURE 6-16.

The holes join to the sea.

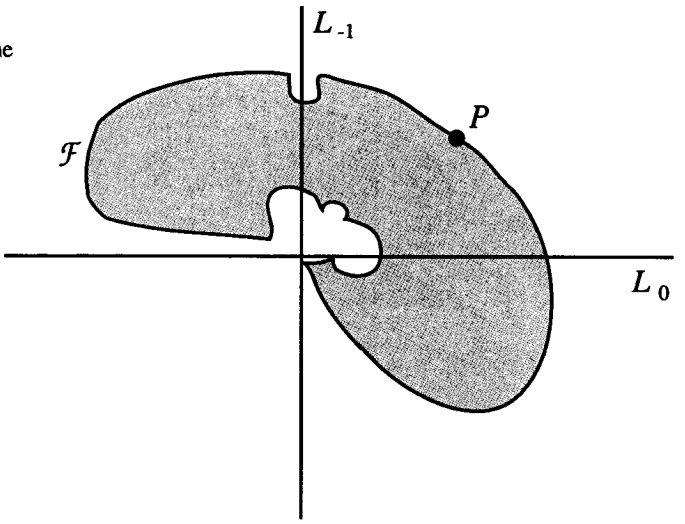

6.2 EXEMPLARY BIFURCATION SEQUENCE

Here again we use the first family of quadratic maps, this time with $a = -1.5$. As before, this map family has fixed points P and Q, and a repelling 2-cycle, $\{Q_1, Q_2\}$.

As the bifurcation parameter, b, decreases from zero, the fixed point Q changes from an attractor to a repelling focus, giving rise to an attractive invariant closed curve, Γ, which crosses L_{-1}, undergoes several bifurcations, as a result of which there appears an annular absorbing area containing a chaotic attractor.

The fixed point P is now a repelling node of a special kind (which we call a *cusp point*; see Appendix A3.2) on the frontier $\mathcal{F}$, which is the boundary separating two basins, the basin D of an absorbing area d', and its complement, $D(\infty)$, which is the basin of infinity, that is, the set of all points whose trajectories recede to infinity.

In this family of maps, however, new kinds of local and global bifurcations take place on the frontier $\mathcal{F}$. The 2-cycle becomes a repelling node, and undergoes a Myrberg sequence of period-doubling bifurcations, which create an infinity of cycles on F. Also, the cusp point, P, creates a new kind of global bifurcation due to contacts between $\mathcal{F}$ and L. In this situation, the quality of the fractal structure of $\mathcal{F}$ changes from soft to hard, as we shall see. We are going to decrease b from -1.5 to -2.115, in 12 stages.

Stage 1: $b = -1.50000$

The basin D begins life as the basin of attraction of the fixed point Q, while it is still attracting. Here, as shown in Figure 6-17, there is a first contact between $\mathcal{F}$, the boundary of D, and L. The rank 1 preimage of P, the point P_{-1}, crosses L, moving from zone Z_0 to Z_2. After this contact bifurcation, the basin D is disconnected.

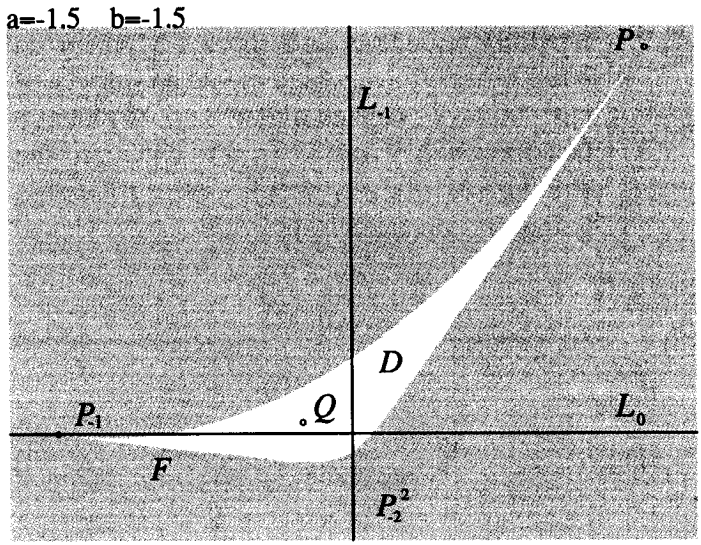

FIGURE 6-17.

Contact bifurcation.

Stage 2: $b = -1.59000$

In Figure 6-18, after contact, we see that D has two components, the immediate basin, D_0, and a component belonging to the zone Z_0, D_{-1}, and thus having no preimages. This first contact bifurcation has disconnected the basin, D, and is of one of the types described in Figure 6-2, or equivalently, Figure 6-9. Note that the fixed point Q is now repelling, and has emitted an attractive invariant closed curve, Γ. Recall that the regions R_1 and R_2 are folded onto the zone Z_2 by the map.

FIGURE 6-18.

After contact. Note the small island.

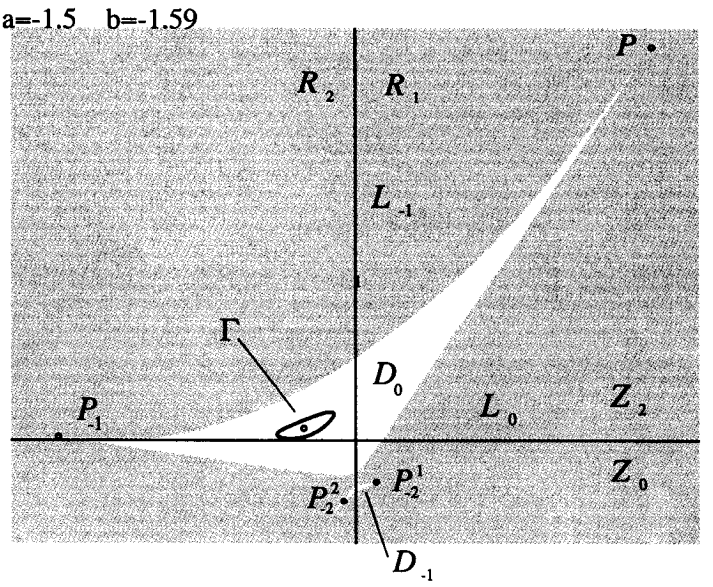

Stage 3: $b = -1.60100$

The second contact bifurcation occurs at this value. As shown in Figure 6-19, the two components of D are reunited, and D again becomes connected. The closures of D_0 and D_{-1} meet at the point k_{-1} of L_{-1}. Note that an arc of the frontier of D_0 is tangent to L at k_0.

FIGURE 6-19.

Second contact.

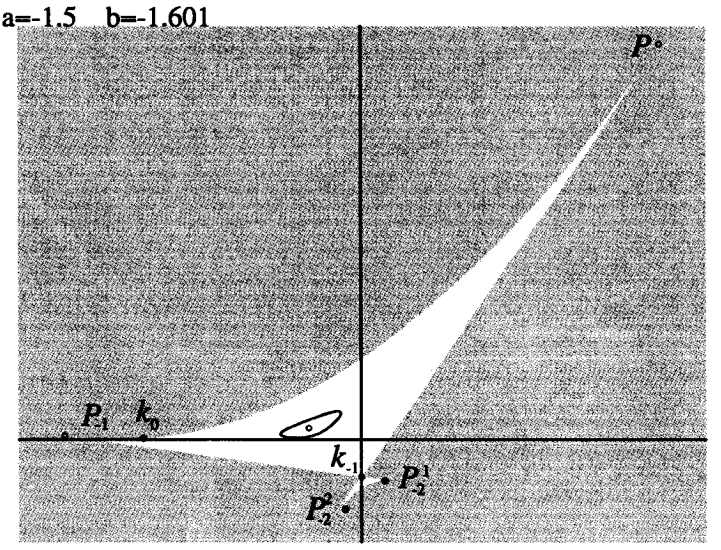

Stage 4: $b = -1.75000$

In Figure 6-20, after the second contact bifurcation, the basin D is again connected, due to the reunion of the two components. This is an instance of the contact bifurcation described in Figures 6-9, 6-10, and 6-11.

These first four stages comprise exactly the sequence of Figures 6-7 to 6-11 of Section 6.1. The next stages comprise the sequence of Figures 6-12 to 6-16 of Section 6.1.

FIGURE 6-20.

After the second contact.

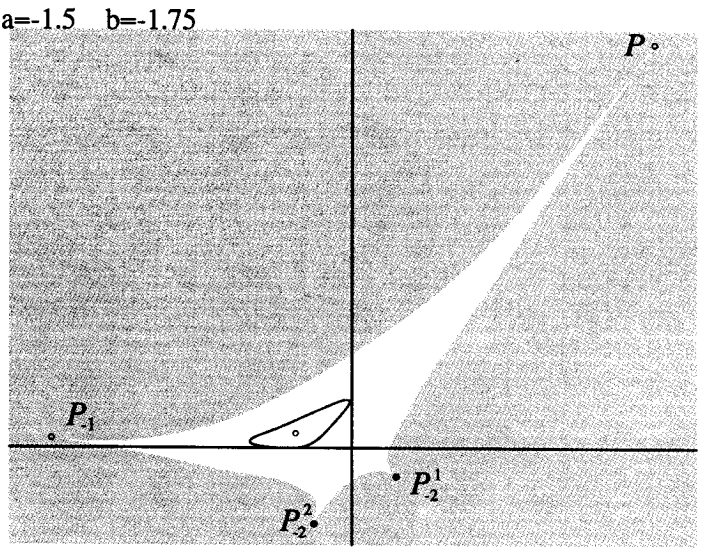

Stage 5: $b = -1.95021$

In Figure 6-21, we see that the boundary of D, coming from Z_0, has made contact with L at h_0, exactly as in Figure 6-13.

FIGURE 6-21.

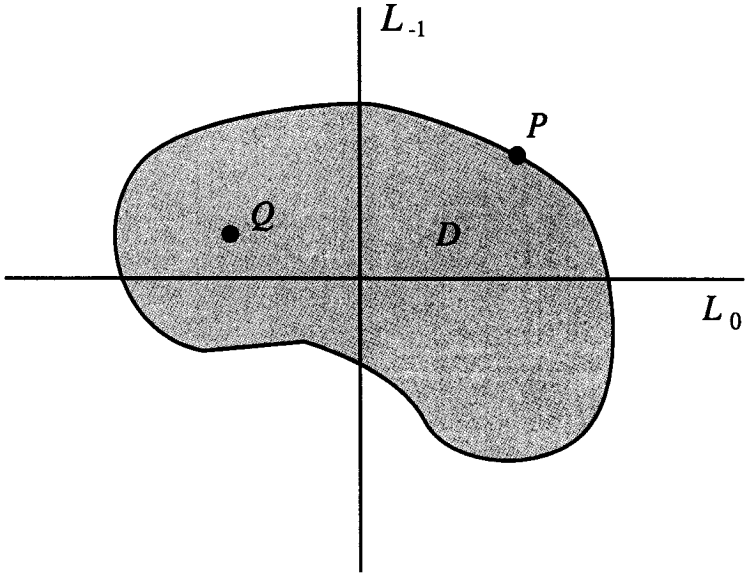

Stage 6: $b = -1.95500$

In Figure 6-22, we see the main hole, H_{-1}. Infinitely many sequences of holes also exist. At lower values of b, these holes become wider, and there are sequences of bifurcations like those already observed in the map family of Chapter 5. That is, holes crossing from Z_0, through L, into Z_2 cause other explosions of sequences of preimages. And holes crossing from Z_2, through L, into Z_0 cause reunions of holes.

Remark. This situation differs from that of the preceding chapter, in which the holes, preimages of H_{-1}, have only two accumulation points (the repelling focus and its rank 1 preimage.) But here, the preimages of H_{-1} accumulate on several repelling cycles belonging to $\mathcal{F}$.

FIGURE 6-22.

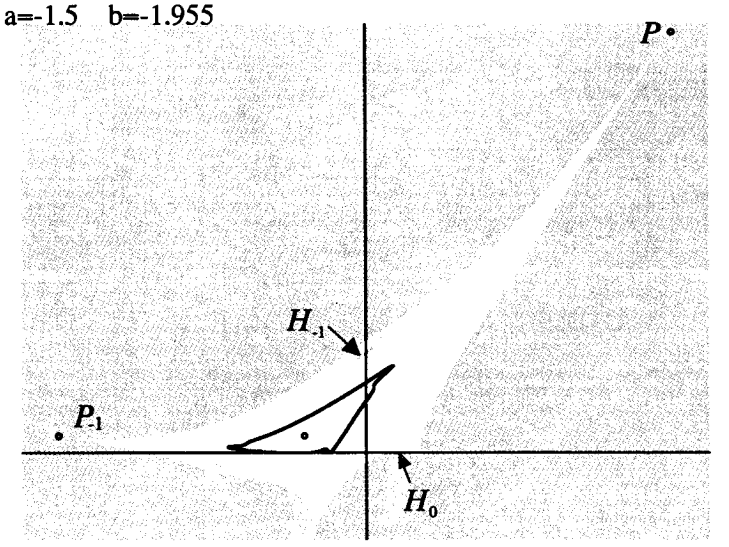

Stage 7: $b = -1.98000$

We will now see that the hole sequences have a self-similar structure: in successive enlargements, similar structures will be observed. In Figure 6-23, we see the two basins, D and $D(\infty)$, in a large domain of the plane. The hole H_{-1} and its two preimages of rank 1 are indicated. Note, for future reference, the rectangle drawn around H_{-1}. Some of the cusp points, the fixed point P and its preimages, are indicated also.

Figure 6-24 is an enlargement of the small rectangle drawn in Figure 6-23. Figure 6-25 to 6-27 are successive enlargements of the indicated rectangles, the self-similarity of the holes is evident. We call this structure a *weak fractal*. The frontier, $\mathcal{F}$, has a weak fractal structure caused by the accumulation on the interior boundary, $\mathcal{F}_i$, of preimages of the main hole, H_{-1}. The fractal structure is weak in the sense that there are only a finite number of cusp points on the frontier. This will change in the next bifurcation. As b decreases further, all the holes approach each other, and all approach the external boundary, $\mathcal{F}_e$.

Figure 6-28 is an instance of the bifurcation shown in Figure 6-15, in which the holes meet each other and the frontier.

FIGURE 6-23.

The big picture.

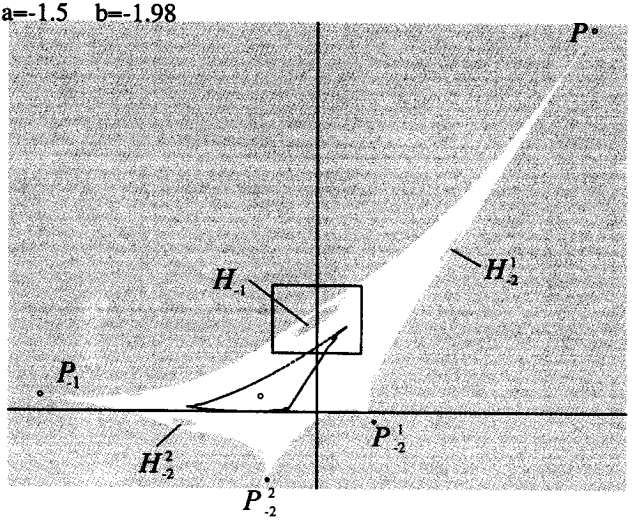

FIGURE 6-24.

First enlargement.

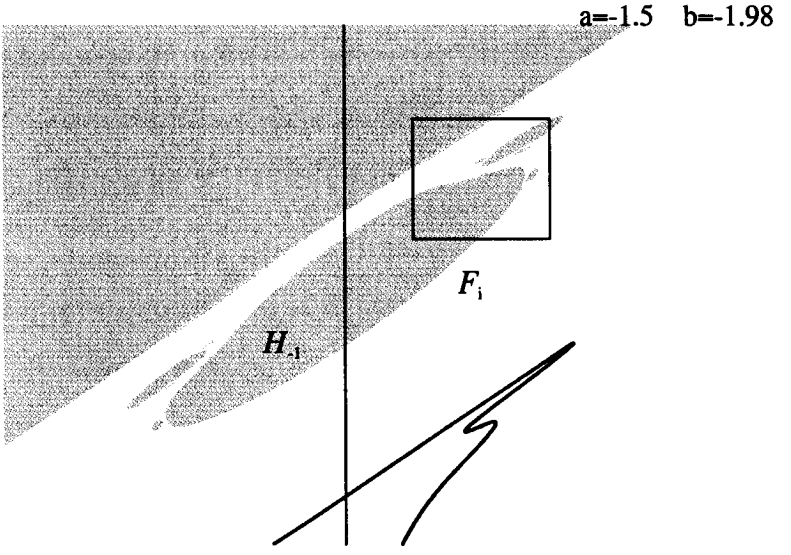

FIGURE 6-25.

Second enlargement.

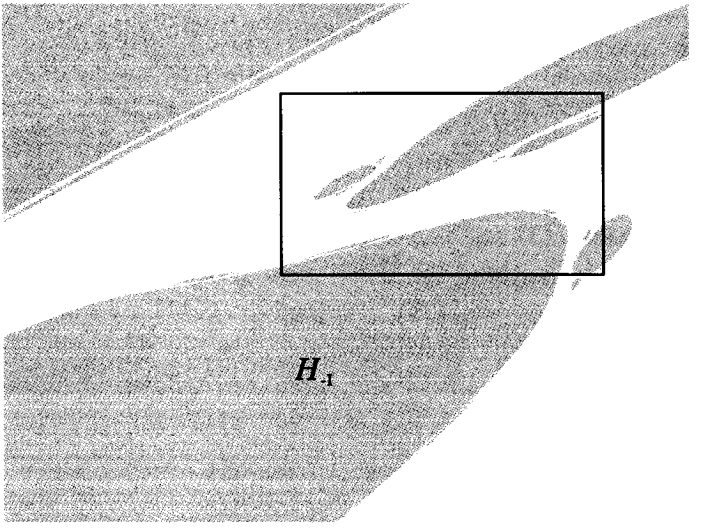

FIGURE 6-26.

Third enlargement.

a=-1.5 b=-1.98

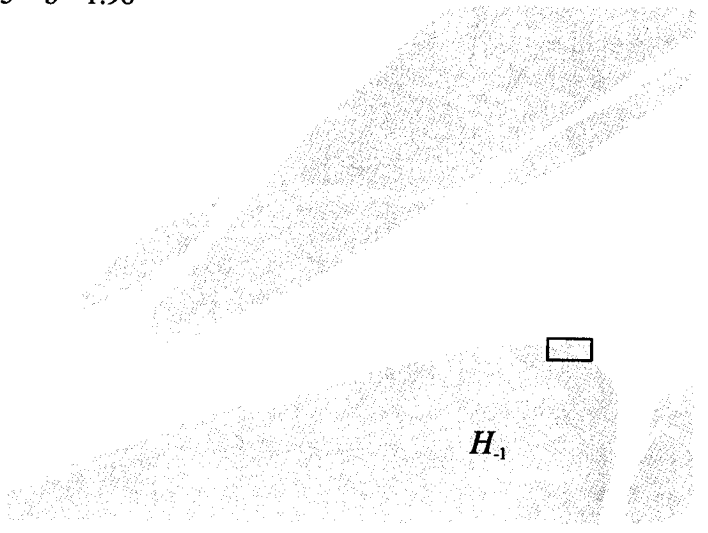

FIGURE 6-27.

Fourth and final enlargement.

a=-1.5 b=-1.98

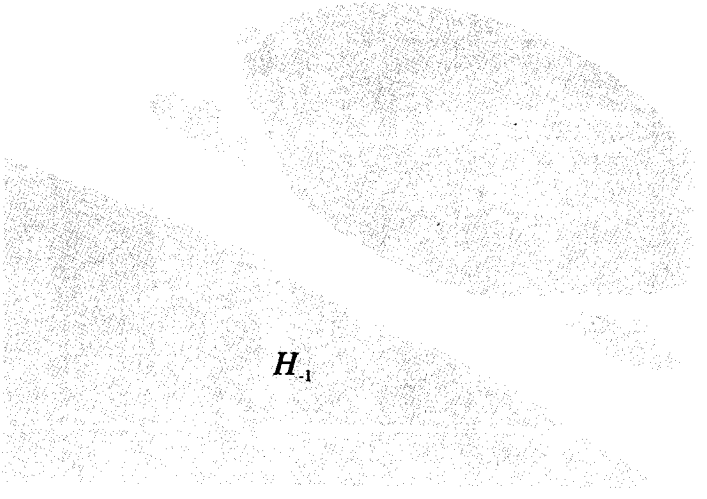

FIGURE 6-28.

Note the new hole, darkly shaded.

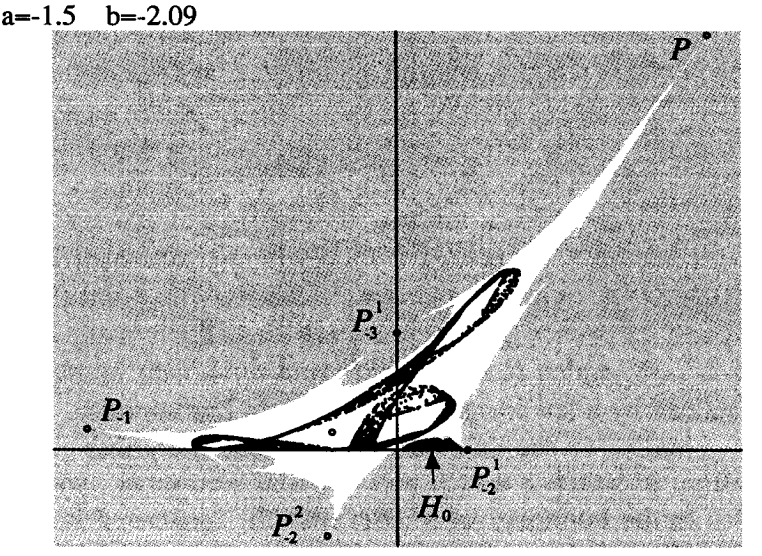

Stage 8: *b* = – 2.09000

The attractor has exploded.

Stage 9: b = – 2.10000

Figure 6-29 shows that the cusp point, $P^1{}_{-2}$, has moved from zone Z_0, through L, into Z_2. All the holes which are preimages of the main hole, H_{-1}, have disappeared. They are now connected to the basin of infinity, $D(\infty)$. An explosion of arborescent sequences of preimages of the cusp point P has created an infinity of cusp points on the external frontier $\mathcal{F}_e$, which now has a strong fractal structure: now there are infinitely many cusps.

Here is a mechanism which might be involved in this bifurcation: Some cusps on the frontier near L may leave headlands, preimages of which are islands inside former holes. An example

(before, during,. and after) is shown in Figure 6-30, in which a portion the basin, D, is shown shaded. In this hypothetical situation, the total basin, D, is not connected.

However, in our case the basin D is simply connected, that is, has no holes. This is shown in Figure 6-31, in which the basin D is white and the basin of infinity, $D(\infty)$, is shaded. Note that the black chaotic area, which is multiply connected, and the absorbing area to which it belongs, are near the frontier, $\mathcal{F}$, which separates the two basins. The hole $W(Q)$ contains the repelling fixed point, Q. The three holes labelled W_1, W_2, and W_3, surround a repelling 3-cycle.

It is clear that there is a simply connected absorbing area, d', containing the chaotic attractor, within D. The point $(0, -1.99)$ in L_1 and the point $(0, -1.2)$ in L_2 are the endpoints of a line segment in L_{-1}, S, which is shown in Figure 6-31. The boundary of d' is obtained by a few images of this straight line segment, S.

Finally, we see that we are approaching another contact bifurcation, in which F and L will touch at a point h_0, which belongs also to the boundary of d'. Because the frontier $\mathcal{F}$ is a fractal, or fuzzy, it will be difficult to determine the exact moment of this contact. Figure 6-32 is an enlargement of the lower left rectangle in Figure 6-31, while Figure 6-33 is an enlargement of the rectangle on the right of Figure 6-31. These two enlargements clearly show the approaching contact of $\mathcal{F}$ and L.

The contact of $\mathcal{F}$ and L may be detected by examining the successive images of the segment, S. As long as they belong to d', the bifurcation has not yet occurred.

Stage 10: $b = -2.10300$

Here at last is the contact between $\mathcal{F}$ and L. Figure 6-34 shows the arc of L which is involved in the contact at the point h_0. It is part of the boundary of the image of W_1, and is the image of a small segment of L_{-1} inside W_1. This segment contains the point h_{-1}. The main hole, H_{-1}, will appear in W_1.

FIGURE 6-29.

A cusp point crossing L, the horizontal line.

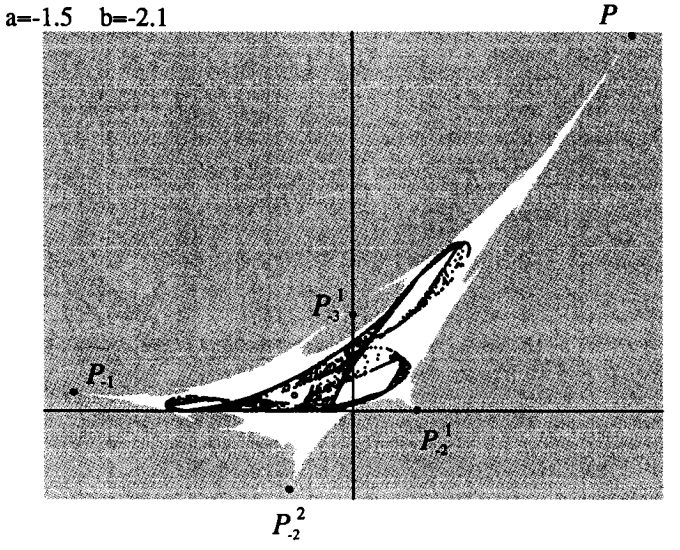

FIGURE 6-30.

Before, during, and after the hypothetical bifurcation. The cusp point moves up through L, while at the same time, a hole merges with the headland.

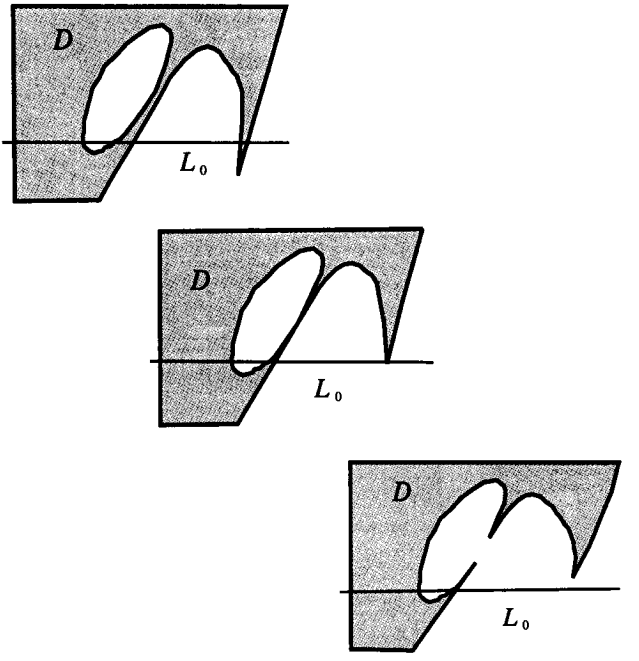

FIGURE 6-31.

The holes, the segment S, and two windows to be enlarged. In these windows, a contact event like that of the preceding figure (or some close relative) is occurring.

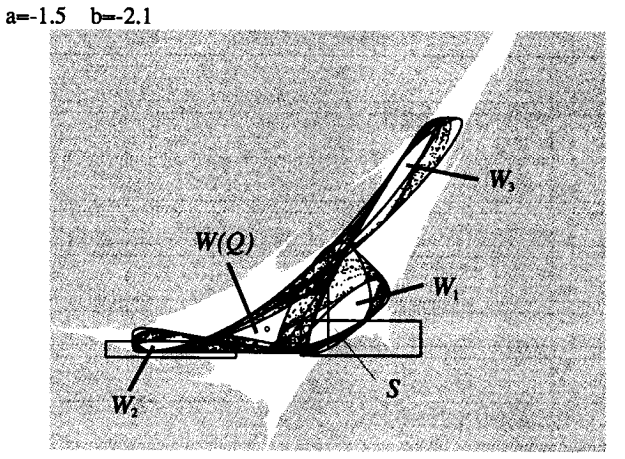

FIGURE 6-32.

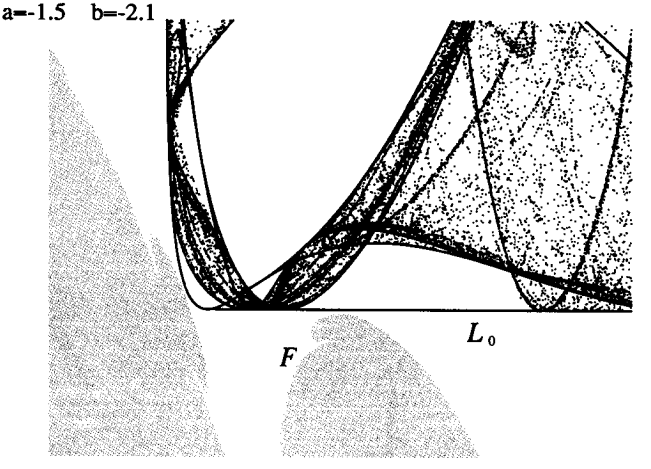

FIGURE 6-33.

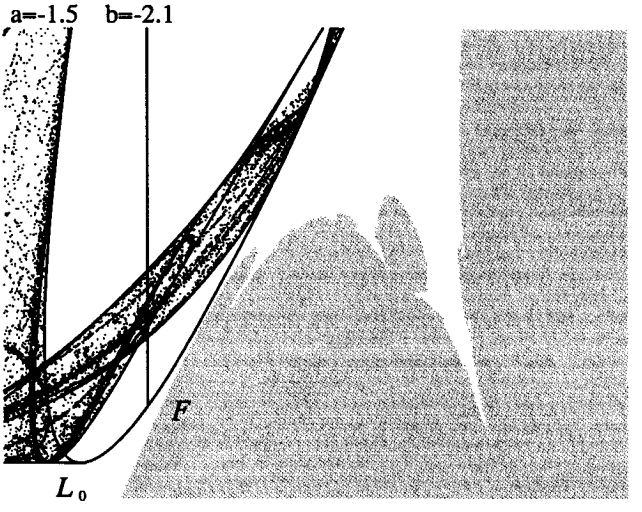

FIGURE 6-34.

The frontier F approaching the horizontal segment of L in the lower left. Its preimage is the short vertical segment in the white hole on the right.

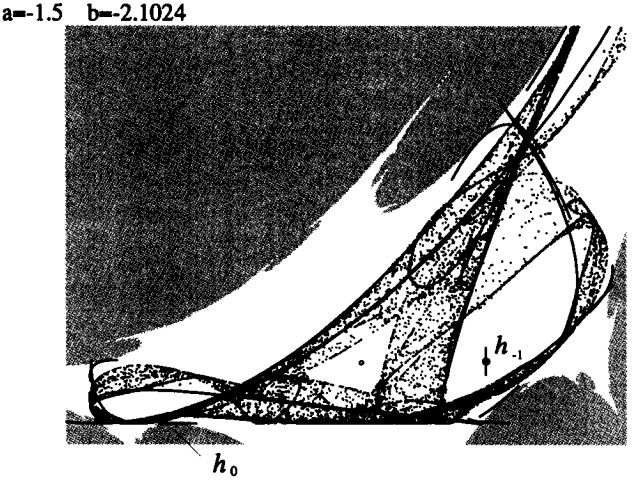

Stage 11: $b = -2.11000$

Figure 6-35 gives an overall view of the two basins, after the bifurcation at Stage 10. Figures 6-36 and 6-37 are enlargements of two different rectangular areas, showing holes inside the regions W_2 and W_1, respectively. Figure 6-38, the enlargement of the third rectangle (upper) shown in Figure 6-35, shows the fractal structure of the holes: close to the boundary, there are more and more holes.

An invariant chaotic area, bounded by a finite number of critical arcs, still exists. As b decreases further, however, the holes become wider and approach the chaotic area. Somewhere, a hole is approaching L near a critical arc of the boundary of the chaotic area.

FIGURE 6-35.

The big picture. Compare with Figure 6-31.

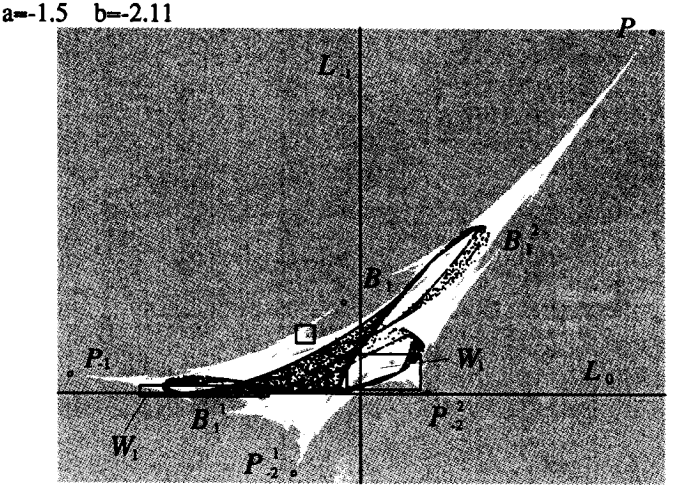

FIGURE 6-36.

Enlargement of the lower left rectangle.

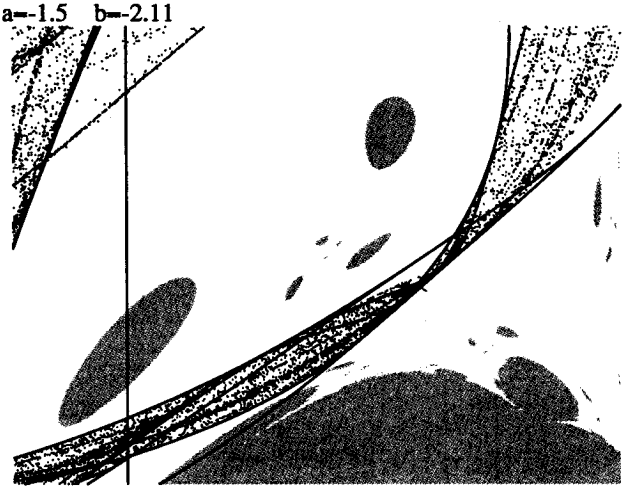

FIGURE 6-37.

Enlargement of the lower right rectangle.

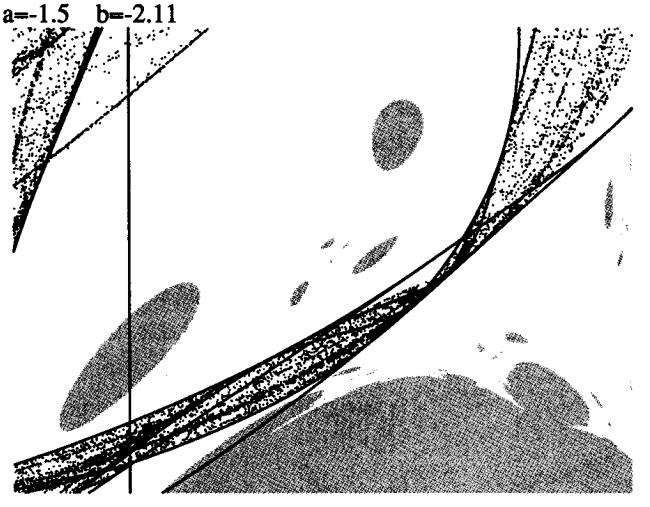

FIGURE 6-38.

Enlargement of the upper rectangle.

Stage 12: b = – 2.11300

In Figure 6-39, tongues of the chaotic area have appeared which cross the boundary of the old chaotic area. A bifurcation is approaching, in which these tongues (for example, L_{12} and L_{13}) will become tangent to and then cross the frontier $\mathcal{F}$. This occurs at about $b = -2.11400$.

This is the final contact bifurcation in our sequence, as now the former chaotic area has been pierced with holes and destroyed. That is, it has lost invariance and attractivity.

FIGURE 6-39. a=-1.5 b=-2.113